RESEARCH ARTICLE

Distinct Roles of the Repeat-Containing Regions and Effector Domains of the *Vibrio vulnificus* Multifunctional-Autoprocessing Repeats-in-Toxin (MARTX) Toxin

Byoung Sik Kim, Hannah E. Gavin, Karla J. F. Satchell

Department of Microbiology-Immunology, Feinberg School of Medicine, Northwestern University, Chicago, Illinois, USA

ABSTRACT ***Vibrio vulnificus*** **is a seafood-borne pathogen that destroys the intestinal epithelium, leading to rapid bacterial dissemination and death. The most important virulence factor is the multifunctional-autoprocessing repeats-in-toxin (MARTX) toxin comprised of effector domains in the center region flanked by long repeat-containing regions which are well conserved among MARTX toxins and predicted to translocate effector domains. Here, we examined the role of the repeat-containing regions using a modified *V. vulnificus* MARTX ($MARTX_{Vv}$) toxin generated by replacing all the internal effector domains with β-lactamase (Bla). Bla activity was detected in secretions from the bacterium and also in the cytosol of intoxicated epithelial cells. The modified $MARTX_{Vv}$ toxin without effector domains retained its necrotic activity but lost its cell-rounding activity. Further, deletion of the carboxyl-terminal repeat-containing region blocked toxin secretion from the bacterium. Deletion of the amino-terminal repeat-containing region had no effect on secretion but completely abolished translocation and necrosis. Neither secretion nor translocation was affected by enzymatically inactivating the cysteine protease domain of the toxin. These data demonstrate that the amino-terminal and carboxyl-terminal repeat-containing regions of the $MARTX_{Vv}$ toxin are necessary and sufficient for the delivery of effector domains and epithelial cell lysis *in vitro* but that effector domains are required for other cytopathic functions. Furthermore, Ca^{2+}-dependent secretion of the modified $MARTX_{Vv}$ toxin suggests that nonclassical RTX-like repeats found in the carboxyl-terminal repeat-containing region are functionally similar to classical RTX repeats found in other RTX proteins.**

IMPORTANCE **Up to 95% of deaths from seafood-borne infections in the United States are due solely to one pathogen, *V. vulnificus*. Among its various virulence factors, the $MARTX_{Vv}$ toxin has been characterized as a critical exotoxin for successful pathogenesis of *V. vulnificus* in mouse infection models. Similarly to MARTX toxins of other pathogens, $MARTX_{Vv}$ toxin is comprised of repeat-containing regions, central effector domains, and an autoprocessing cysteine protease domain. Yet how each of these regions contributes to essential activities of the toxins has not been fully identified for any of MARTX toxins. Using modified $MARTX_{Vv}$ toxin fused with β-lactamase as a reporter enzyme, the portion(s) responsible for toxin secretion from bacteria, effector domain translocation into host cells, rapid host cell rounding, and necrotic host cell death was identified. The results are relevant for understanding how $MARTX_{Vv}$ toxin serves as both a necrotic pore-forming toxin and an effector delivery platform.**

Received 4 March 2015 **Accepted** 10 March 2015 **Published** 31 March 2015

Citation Kim BS, Gavin HE, Satchell KJF. 2015. Distinct roles of the repeat-containing regions and effector domains of the *Vibrio vulnificus* multifunctional-autoprocessing repeats-in-toxin (MARTX) toxin. mBio 6(2):e00324-15. doi:10.1128/mBio.00324-15.

Editor Jeff F. Miller, UCLA School of Medicine

Address correspondence to Karla J. F. Satchell, k-satchell@northwestern.edu.

This article is a direct contribution from a Fellow of the American Academy of Microbiology.

The pathogenic estuarine bacterium *Vibrio vulnificus* is the causative agent of gastroenteritis, necrotizing fasciitis, and life-threatening septicemia resulting both from consumption of contaminated seafood and from wound infections in immunocompromised individuals (1–4). Disease caused by infection with *V. vulnificus* is notable for its invasive nature, severe tissue damage, and high mortality rate, which is dependent on the health status of the host and the time before onset of health intervention (5).

Among numerous virulence factors, the *V. vulnificus* multifunctional-autoprocessing repeats-in-toxin ($MARTX_{Vv}$) toxin encoded by the 15.6-kb *rtxA1* gene is one of the most important for *V. vulnificus* pathogenesis by both the intestinal and wound routes of infection (6–11). The toxin functions additively, along with the VvhA cytolytic/hemolysin pore-forming toxin, to induce rapid *in vivo* growth, destruction of epithelial tissue, massive inflammation, and death (6, 7, 12). The 5,206-amino-acid (aa) $MARTX_{Vv}$ toxin from representative clinical isolate CMCP6 (13) is a composite toxin comprised of repeat-containing regions and five centrally located effector domains (Fig. 1A) (14, 15). The repeat-containing regions include an ~200-kDa amino-terminal arm, >50% of which consists of 19-to-20-aa glycine-rich repeats, and an ~100-kDa carboxyl-terminal arm containing additional glycine-rich repeats and 15 copies of an atypically structured 18-aa RTX repeat. Adjacent to the C-terminal repeat regions is the inositol hexakisphosphate ($InsP_6$)-inducible cysteine protease do-

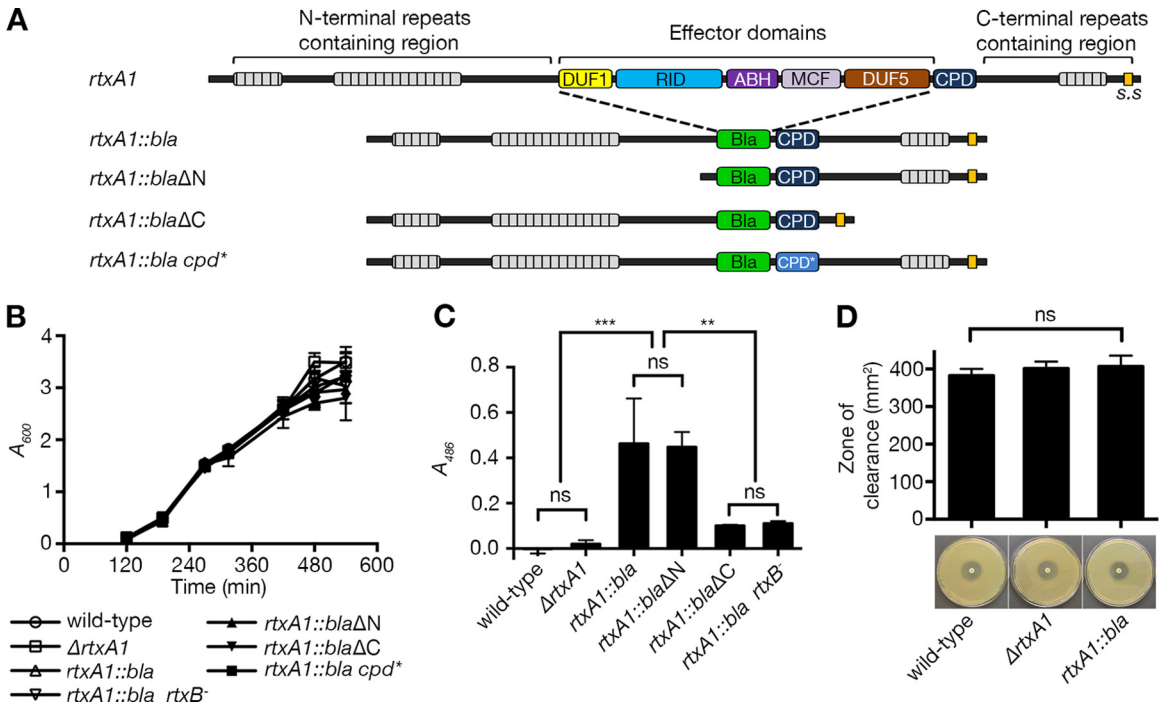

FIG 1 Modification of $MARTX_{Vv}$ toxin does not affect bacterial growth and toxin secretion except for carboxyl-terminal repeat-containing region truncation. (A) Schematic diagrams showing the toxin produced from the *rtxA1* gene from the wild-type strain with the 5 known effector domains (14–16): domain of unknown function in the first position (DUF1), Rho-inactivation domain (RID), alpha-beta hydrolase enzyme (ABH), make caterpillars floppy homology domain (MCF), and domain of unknown function in the fifth position (DUF5). The toxin produced by the strain with the modified *rtxA1*::*bla* gene retains the repeat-containing regions (grey hatched bars), the C-terminal secretion signal (*s.s*), the cysteine protease domain (CPD; black), and natural CPD processing sites but delivers Bla (green) in place of the normal five effector domains. Additional ΔN and ΔC deletion mutants express truncated toxins as depicted. Nonfunctional CPD* (light blue) is indicated. (B) Growth curves in LB broth show no growth defect for the strains with the modified *rtxA1* gene. (C) Secretion of modified $MARTX_{Vv}$ toxin from the indicated strain was examined by nitrocefin cleavage assay using whole bacterial culture. (D) Assessment of susceptibility of the indicated strains to ceftazidime. Statistical significance was determined by multiple comparisons after one-way analysis of variance (ANOVA) (**, $P < 0.005$; ***, $P < 0.001$; ns, not significant).

main (CPD) essential for toxin autoprocessing to release the effector domains localized between the N-terminal arm and CPD to the cytosol (Fig. 1A) (16). Although no structural analysis has been performed, the repeats in the arms are suggested to form a pore or pore-like structure in the epithelial cell membrane for translocation of the CPD and the effector domains, with autoprocessing then occurring in the $InsP_6$-rich eukarytoic cell cytosol (16, 17).

The $MARTX_{Vv}$ holotoxin has both cytotoxic and cytopathic effects on eukaryotic cells, including necrosis, apoptosis, induction of reactive oxygen species, actin depolymerization, and pyroptosis (11, 18–21). The effector domains have been proposed to be mediators of some of these toxicities (14, 16). Indeed, modification of the effector domain repertoire has been shown to affect virulence in mice (14). In contrast, a recent study using toxin fragments ectopically expressed within the eukaryotic cell cytosol suggested that the CPD plus the carboxyl-terminal repeat-containing region is sufficient for necrosis of cells (19). This fragment, however, was not sufficient to induce cell lysis when purified and added exogenously to cells (22). Together, these findings lead to the issue of whether the translocated effector domains or properties of the repeat-containing regions are responsible for cytotoxic and/or cytopathic effects of the $MARTX_{Vv}$ toxin.

To separate the function of repeat-containing regions from that of the effector domains, we constructed a *V. vulnificus* strain in which the *rtxA1*-encoded $MARTX_{Vv}$ toxin is modified to deliver a heterologous reporter enzyme β-lactamase (Bla) in place of the effector domains. The modified $MARTX_{Vv}$ toxin retained the ability to be secreted from the bacterium (dependent upon Ca^{2+}), to translocate domains into epithelial cells, and to lyse epithelial cells. The delivery of domains from bacteria to host cell cytosol, as well as the cell lysis, requires both the amino- and carboxyl-terminal repeat-containing regions of the toxin but not the CPD. Overall, the repeat-containing regions have been found to confer *in vitro* necrotic cell death when the toxin is naturally delivered from bacteria but cannot account for all activities of the toxin, indicating that the effector domains also contribute to toxic action.

RESULTS

A modified $MARTX_{Vv}$ toxin with effector domains replaced with Bla. In order to delineate the function of independent portions of the toxin during natural intoxication of cells, a method is needed to ensure that genetic modification of the *rtxA1* toxin gene does not also disrupt protein synthesis, secretion from the bacterium, surface binding, or translocation. We established a system in which the effector domains were replaced with the mature *Escherichia coli* TEM-1 Bla as an in-frame fusion (23–25), while the natural CPD autoprocessing site at aa 4090 (as mapped by Shen et al. [17]) and the putative processing site in front of domain of

TABLE 1 Plasmids and bacterial strains used in this study

Strain or plasmid	Relevant characteristics[a]	Reference or source
Strains		
V. vulnificus CMCP6	Clinical isolate; virulent, Rif^r	6
V. vulnificus BS1405	CMCP6 Δ*vvhA*, Rif^r	This study
V. vulnificus BS1406	BS1405 Δ*rtxA1*, Rif^r	This study
V. vulnificus BS1407	BS1405 *rtxA1*::*bla*, Rif^r	This study
V. vulnificus BS1408	BS1405 *rtxA1*::*bla*ΔN, Rif^r	This study
V. vulnificus BS1409	BS1405 *rtxA1*::*bla*ΔC, Rif^r	This study
V. vulnificus HEG1407	BS1407 *cpd**, Rif^r	This study
V. vulnificus BS1416	BS1407 *rtxB*::*nptII*, Km^r, Rif^r	This study
E. coli SM10λpir	*thi thr leu tonA lacY supE recA*::RP4-2-Tc::Muλ*pir*; Km^r	49
E. coli S17-1λpir	*thi pro hsdR hsdM+ recA*::RP4-2-Tc::Mu-km::Tn*7*; λ*pir*; Sm^r	50
Plasmids		
pBlueScript-II	Cloning vector containing *bla*; Ap^r	Stratagene
pKanπ	Kanamycin cassette-containing vector, Km^r	Laboratory collection
pDS132	*oriR6K*, *sacB*; *oriTRP4*; Cm^r	48
pBS1311	Δ*vvhA* in pDS132; Cm^r	This study
pHGJ5	*rtxA1*::*bla* in pDS132; Cm^r	This study
pBS1347	*rtxA1*::*bla*ΔN in pDS132; Cm^r	This study
pBS1348	*rtxA1*::*bla*ΔC in pDS132; Cm^r	This study
pHEG1401	*rtxA1*::*bla*::*cpd** in pDS132; Cm^r	This study
pBS1438	*rtxB*::*nptII* in pDS132; Km^r, Cm^r	This study

[a] Rif^r, rifampin resistant; Km^r, kanamycin resistant; Sm^r, streptomycin resistant; Cm^r, chloramphenicol resistant; Ap^r, ampicillin resistant; *cpd**, catalytically inactive, nonfunctional *cpd*.

unknown function in the first position (DUF1) (after aa 1959 based on alignment to the known processing site for *V. cholerae* MARTX [$MARTX_{Vc}$] [26]) were retained (Fig. 1A). The modified gene arrangement was exchanged into the chromosome of *V. vulnificus* CMCP6 strain by double homologous recombination to create an *rtxA1*::*bla* strain. Because hemolysin also has a role in cytolysis (12, 27), the *vvhA* gene was further deleted from all strains used in this study (Table 1); therefore, the Δ*vvhA* strain is referred to as the wild-type strain here. The growth rates in broth media of the *rtxA1*::*bla* strain and further modified strains were identical to those of the wild-type and Δ*rtxA1* strains, indicating that the modification to *rtxA1* did not affect *V. vulnificus* growth *in vitro* (Fig. 1B).

The $MARTX_{Vv}$ toxin modified to carry Bla is secreted to culture media. First, secretion of the toxin from bacteria was assessed. The unmodified $MARTX_{Vv}$ toxin is known to be secreted to culture media by a dedicated Type I secretion apparatus (28). After secretion, the toxin is rapidly degraded such that only fragments of the toxin remain (10, 19, 28); thus, spent cell-free supernatant fluids lack $MARTX_{Vv}$-associated cytolytic activity (11). Despite this degradation, we surmised that a stable Bla fragment might remain active, allowing quantification of toxin secretion. Indeed, whole-cell culture of the *rtxA1*::*bla* strain, but not of the wild-type or the Δ*rtxA1* strain, was able to hydrolyze the chromogenic Bla substrate nitrocefin (Fig. 1C).

The *rtxA1*::*bla* strain was further modified to introduce a polar insertion into the *rtxB* gene to disrupt the entire *rtxBDE* type I secretion system (TISS) operon. The bacterial cell culture of the resulting *rtxA1*::*bla* strain with the *rtxB* insertion could not hydrolyze nitrocefin, indicating that the Bla activity in the whole-cell culture of *rtxA1*::*bla* strain was due to the presence of secreted $MARTX_{Vv}$ toxin (Fig. 1C).

Since the third-generation β-lactam antibiotic ceftazidime is recommended for the treatment of *V. vulnificus* infections in humans (29), we also tested whether the modification rendered the strain resistant to ceftazidime using an antibiotic disk assay. The modified strain was not resistant to ceftazidime (Fig. 1D), which is consistent with data indicating that the TEM1 Bla is not able to cleave this antibiotic *in vitro* (30); thus, the strain encoding the modified toxin poses no increased biohazardous risk compared to the parent strains.

The $MARTX_{Vv}$ toxin repeat-containing regions are sufficient for heterologous translocation of Bla to eukaryotic cell cytosol. Next, HeLa cervical carcinoma cells were incubated with *V. vulnificus* and subsequently loaded with the membrane-permeant coumarin cephalosporin fluorescein reagent CCF2/AM (24). After uptake into cells, CCF2/AM is de-esterified into its negatively charged form, CCF2, a chemically synthesized variant of the β-lactam antibiotic cephalosporin linked to two fluorophores that can undergo fluorescence resonance energy transfer (FRET). When Bla is present in the cell cytosol, FRET is disrupted. Change in the fluorescence readout from green (CCF2 and FRET intact) to blue (CCF2 cleaved, FRET disrupted) thereby serves as an assay for translocation of Bla into cell cytosol. As de-esterification to CCF2 in the eukaryotic cytosol is required for fluorescence, extracellular toxin is not detected.

About 98.5% ± 0.7% of HeLa cells either left untreated or treated with the Δ*rtxA1* strain emitted only green fluorescence, indicative of FRET, demonstrating uptake and de-esterification of CCF2/AM. In cell cultures treated with the *rtxA1*::*bla* strain for 90 min at a multiplicity of infection (MOI) of 10, 87.7% ± 2.1% of HeLa cells emitted blue fluorescence, indicating that the Bla protein was translocated to the cell cytosol, where it disrupted the FRET (Fig. 2). This translocation was highly efficient because cells positive for Bla translocation (Bla^+ cells) were detected in cells treated at an MOI as low as 2 and as soon as 30 min after the addition of bacteria (Fig. 2). Furthermore, translocation occurred in both an MOI-dependent and a time-dependent manner. These

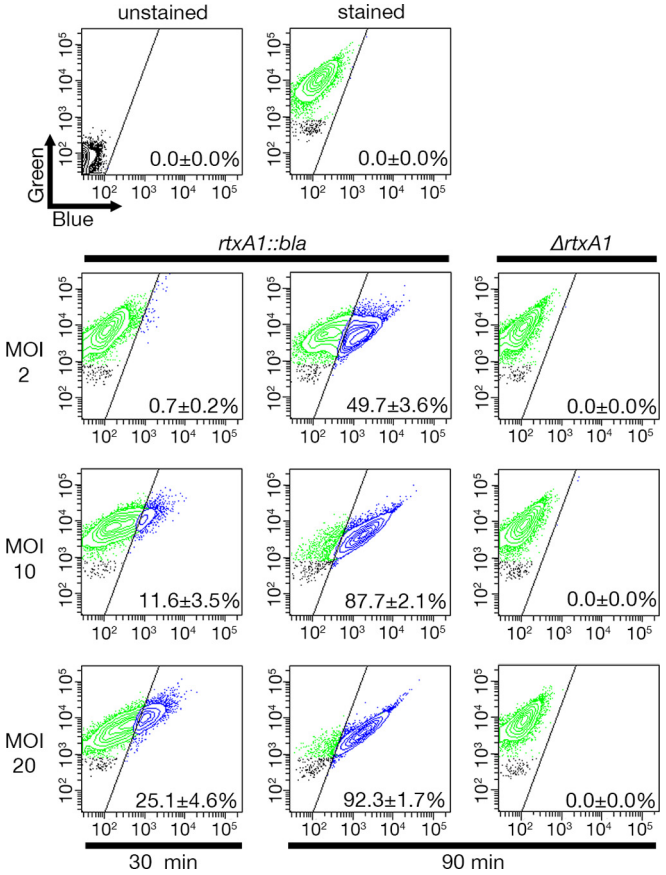

FIG 2 Translocation of Bla into the host cell cytosol by modified $MARTX_{Vv}$ toxin. HeLa cells were incubated with *V. vulnificus* strains as indicated before being loaded with CCF2/AM for 30 min. Translocation of Bla was detected by flow cytometry, where green fluorescence (518 nm; *y* axis) under conditions of violet laser excitation (409 nm) indicates the number of cells loaded with CCF2 and blue fluorescence (447 nm; *x* axis) indicates the number of cells with cleaved CCF2. Representative FACS analysis images from at least three biological replicates are shown, with means ± standard deviations of percentages of Bla-translocated cells shown within each panel.

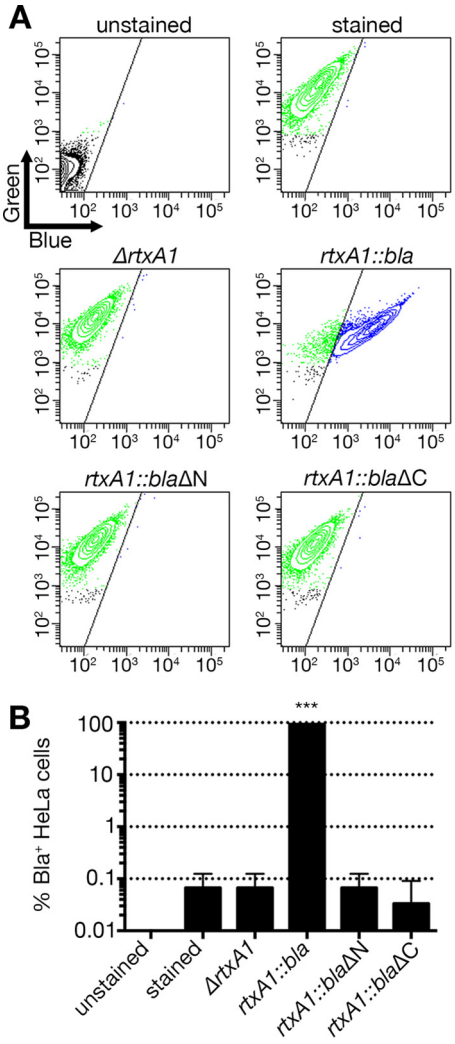

FIG 3 Translocation of Bla by $MARTX_{Vv}$ is not observed in the absence of the N- or C-terminal repeat-containing regions. (A) HeLa cells were treated with the indicated *V. vulnificus* strain at an MOI of 10 for 60 min and then loaded with CCF2/AM. FACS analyses were done as described for Fig. 2, and representative images are shown. (B) Histograms show percentages of Bla-translocated, blue fluorescence-emitting cells as means ± standard deviations ($n \geq 3$). Statistical significance was determined by one-way ANOVA (***, $P < 0.001$).

data demonstrate that Bla present in the central core of the toxin can be secreted and delivered to the eukaryotic cytosol. Further, these data show that the toxin can deliver heterologous peptide sequences.

The carboxyl-terminal repeat-containing regions are required for toxin secretion. Unlike other typical RTX toxins containing nonapeptide repeats, MARTX toxins have an atypically structured 18-aa RTX repeat(s) in the carboxyl-terminal arm. To examine the role of this carboxyl-terminal repeat-containing region, an *rtxA1*::*bla*ΔC strain was generated by removing much of the carboxyl terminus of the *rtxA1*::*bla* sequence (aa 2533 to 3293), leaving gene sequences for the amino terminus, Bla, and CPD intact (Fig. 1A). The extreme carboxyl-terminal secretion signal (ss) for the TISS of the toxin was preserved to rule out any consequence of ss deletion effects. Relative to the *rtxA1*::*bla* strain, the *rtxA1*::*bla*ΔC cultures demonstrated significantly lower Bla activity, comparable to that of the *rtxA1*::*bla* strain with the *rtxB* insertion (Fig. 1C), suggesting that the carboxyl-terminal repeat-containing region has an essential role in $MARTX_{Vv}$ toxin secretion. Consistent with this result, translocation of Bla was not observed in HeLa cells treated with the *rtxA1*::*bla*ΔC strain (Fig. 3).

The amino-terminal repeat-containing regions are required for the Bla translocation. Another unique feature of MARTX toxins compared to typical RTX toxins is the 19- to 20-aa glycine-rich repeat(s) at the amino terminus (Fig. 1A). It has been speculated that these, along with the carboxyl-terminal repeats, may contribute to a pore or pore-like structure for translocation of the central portions of the toxin (16), although this has never been directly demonstrated. To address this issue, an *rtxA1*::*bla*ΔN strain was generated by removing the entire coding region for aa 73 to 1885 of the *rtxA1*::*bla* sequence, such that the expressed toxin would be essentially comprised of Bla linked to the CPD and C terminus (Fig. 1A).

The bacterial cell culture of the *rtxA1*::*bla*ΔN strain showed Bla activity comparable to that of the *rtxA1*::*bla* strain, indicating that the amino terminal repeat-containing region is dispensable for

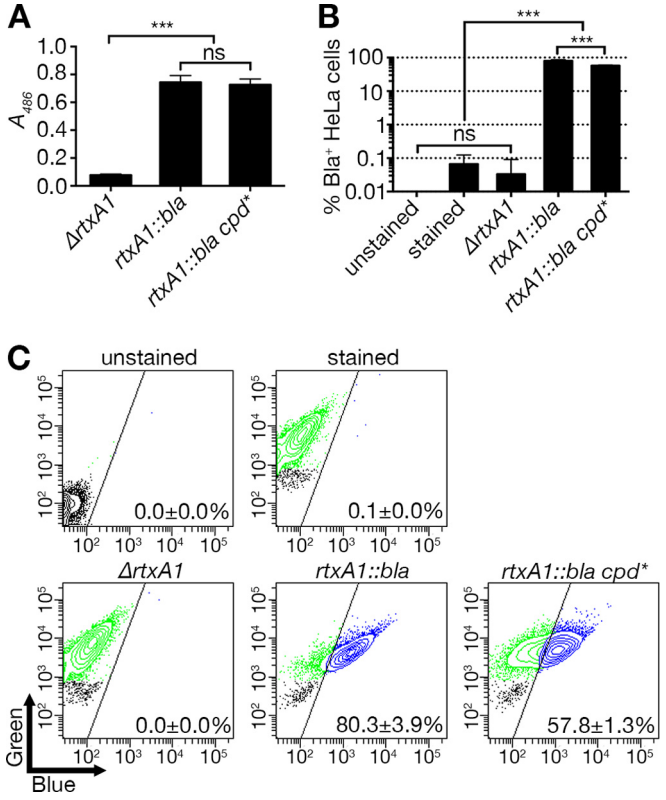

FIG 4 CPD activity is dispensable for MARTX$_{Vv}$ toxin secretion but has a role in Bla translocation efficiency. (A) Modified MARTX$_{Vv}$ toxins as indicated were examined for secretion by nitrocefin cleavage assay. (B) Translocation of Bla domain was measured by *in vitro* translocation assay (means ± standard deviations, $n \geq 3$). (C) Representative FACS data from the translocated HeLa cells. Statistical significance was determined by multiple comparisons after one-way ANOVA (***, $P < 0.001$; ns, not significant).

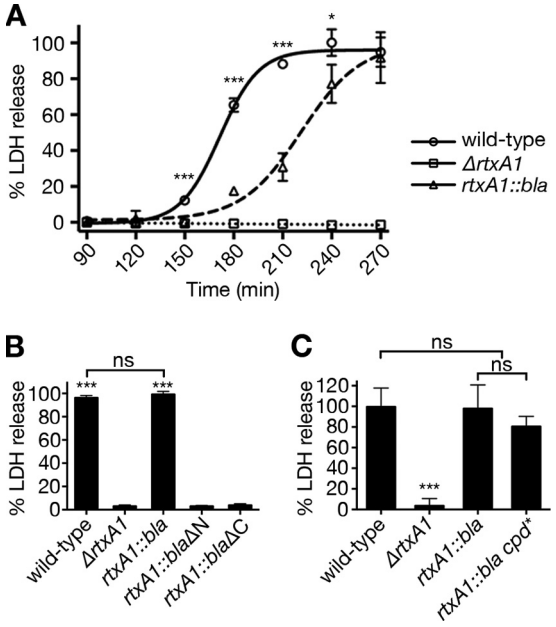

FIG 5 Repeat-containing regions of MARTX$_{Vv}$ toxin are necessary and sufficient for host cell lysis. (A) HeLa cells were coincubated with the indicated *V. vulnificus* strains at an MOI of 10 for the indicated times. LDH release to supernatant fluids was quantified at every 30 min as indicated. The statistical significance of the results of comparisons of the wild-type strain to the *rtxA1*::*bla* strain was determined by Student's *t* test (*, $P < 0.05$; ***, $P < 0.001$). (B and C) Percent HeLa cell lysis at 270 min after coincubation with the indicated *V. vulnificus* strains at an MOI of 10 was determined by LDH release assay. Statistical significance was determined by multiple comparisons after one-way ANOVA (***, $P < 0.001$; ns, not significant).

MARTX$_{Vv}$ toxin secretion (Fig. 1C). However, HeLa cells treated with the *rtxA1*::*bla*ΔN strain did not emit blue fluorescence above the level seen with negative controls, while 92.3% ± 2.2% of HeLa cells treated with the *rtxA1*::*bla* positive-control strain emitted blue fluorescence (Fig. 3). These data demonstrate that the amino-terminal repeat-containing region of MARTX$_{Vv}$ is not required for secretion from the bacterium but is required for Bla translocation into eukaryotic cells during natural intoxication.

The CPD is not necessary for either MARTX$_{Vv}$ toxin secretion or Bla translocation. Another component remaining in the modified MARTX$_{Vv}$ toxin is a CPD that autoprocesses MARTX$_{Vv}$. To test if CPD activity is essential for toxin secretion or translocation, the *rtxA1*::*bla* gene was modified to catalytically inactivate the CPD by incorporating a C4230A point mutation into the *rtxA1* gene. The resulting *rtxA1*::*bla cpd** strain secreted Bla into culture media at levels indistinguishable from those seen with the parent *rtxA1*::*bla* strain (Fig. 4A), indicating that active CPD is not required for toxin secretion.

Further, 57.8% ± 1.3% of HeLa cells treated with the *rtxA1*::*bla cpd** strain emitted blue fluorescence after loading of CCF2/AM (Fig. 4B and C), demonstrating that CPD is not essential for Bla translocation across the membrane to the cytosol. Notably, the number of blue fluorescence-emitting cells was significantly lower than the number seen with the positive-control sample (Fig. 4B). This suggests that active CPD processing of Bla from the holotoxin after translocation increases its activity and the overall detection of Bla$^+$ cells. This is similar to results determined with the *V. cholerae* MARTX toxin (31) and *Clostridium difficile* toxin B (32, 33), where CPD autoprocessing delivery of effector domains to the cytosol is also not essential, although it dramatically increases efficiency and access to larger pools of target and thus becomes essential at lower toxin concentrations.

MARTX$_{Vv}$ repeat-containing regions are responsible for epithelial cell lysis *in vitro*. A critical function of the MARTX$_{Vv}$ holotoxin is the ability to induce necrotic cell death (11, 19) resulting in tissue destruction and bacterial spread (6, 7). The pore formation due to *rtxA1* can be inhibited by addition of polyethylene glycol 3350 to 8000 to media, suggesting the presence of a 1.63-nm pore (11), and pore-dependent activation of caspase 1 is inhibited by the presence of high concentrations of potassium (20). In contrast, release of cellular ATP via P2X7R is not implicated in the response (20). Thus, this is deemed a true pore-dependent necrosis that is easily monitored by release of lactate dehydrogenase (LDH) from cells. To test if the lytic death is caused by the MARTX$_{Vv}$ repeat-containing regions or is instead due to a catalytic action of one of the effector domains, levels of LDH release from bacterium-treated HeLa cells were determined.

HeLa cells incubated with wild-type *V. vulnificus* released LDH after 120 min and reached the maximum level after 240 min (Fig. 5A), while the Δ*rtxA1* negative-control strain showed no LDH release above the control level even by 270 min (Fig. 5A). Experiments performed with the test *rtxA1*::*bla* strain also resulted

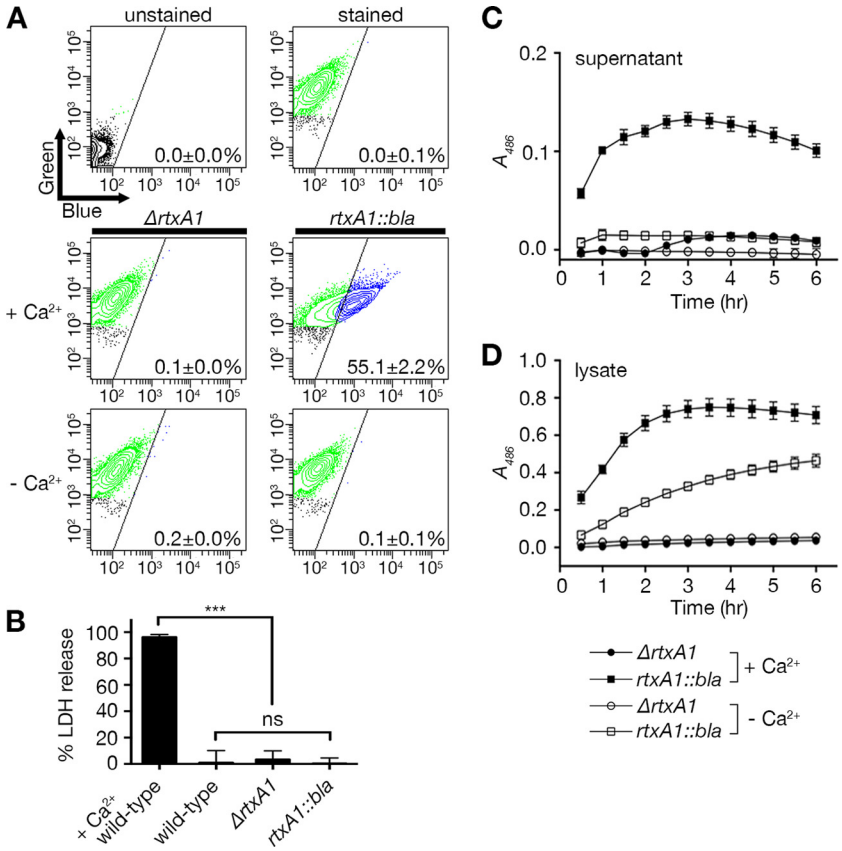

FIG 6 $MARTX_{Vv}$ toxin could not translocate Bla domain or lyse host cells in the absence of Ca^{2+} due to the secretion defect. (A) HeLa cells were treated with the Δ*rtxA1* strain or the *rtxA1*::*bla* strain at an MOI of 10 for 60 min in DMEM with or without 1.8 mM $CaCl_2$ and then loaded with CCF2-AM. FACS analyses were done as described for Fig. 2, and representative images are shown with means ± standard deviations within each panel ($n \geq 3$). (B) Percent HeLa cell lysis determined by LDH release assay as described for Fig. 5B except without Ca^{2+} in DMEM. Data for wild-type strain treated cells in the presence of Ca^{2+} (first bar; $+Ca^{2+}$ wild-type) were adapted from Fig. 5B for comparison. (C and D) Nitrocefin cleavage assay of culture supernatant (C) or total cell lysate (D) from the Δ*rtxA1* strain (circle) or the *rtxA1*::*bla* strain (square) grown statically to mid-exponential phase ($A_{600} = 0.5$) in DMEM with (filled symbols) or without (open symbols) 1.8 mM $CaCl_2$. The absorbance (A_{486}) for nitrocefin cleaved by Bla was measured every 30 min. Data are means ± standard deviations ($n \geq 3$). Statistical significance was determined by multiple comparisons after one-way ANOVA (***, $P < 0.001$; ns, not significant).

in LDH release. This LDH release from the *rtxA1*::*bla*-encoded toxin required the N-terminal repeat region since the *rtxA1*::*bla*ΔN strain did not induce cellular necrosis at all, even by 270 min. As an additional control, the *rtxA1*::*bla*ΔC strain defective for toxin secretion was also assayed and found not to lyse cells (Fig. 5B). The levels of LDH release were also not different between cells treated with the wild-type, *rtxA1*::*bla*, or *rtxA1*::*bla cpd*⋆ strain (Fig. 5C).

Overall, these results indicate that CPD-dependent autoprocessing does not contribute to cellular necrosis and that the repeat-containing regions are sufficient for $MARTX_{Vv}$ toxin-dependent necrotic cell death. However, the LDH release by *rtxA1*::*bla* strain was slightly delayed compared to wild-type strain results (Fig. 5A). Thus, while the repeat-containing regions were sufficient for necrotic cell death, the modification to *rtxA1* to replace the effector domains with Bla did affect the efficiency of lysis, possibly by reducing the levels of toxin secretion, inducing a minor modification to the toxin structure, or by loss of an effector domain that may make a small but additive contribution to lysis.

The absence of cellular necrosis in the absence of Ca^{2+} is due to a lack of toxin secretion from the bacterium. It has previously been shown that the ability of *V. vulnificus* to induce $MARTX_{Vv}$-dependent necrotic cell death requires Ca^{2+} in the media; therefore, it has been postulated that Ca^{2+} is required for programmed necrosis via calcium-dependent mitochondrial pathways (19). Therefore, we tested whether repeat-containing region-dependent host cell lysis also requires extracellular Ca^{2+}. HeLa cells were treated with the Δ*rtxA1* or *rtxA1*::*bla* strain in the presence or absence of Ca^{2+} in Dulbecco's modified Eagle's medium (DMEM). To ensure the absence of Ca^{2+}, Dulbecco's phosphate-buffered saline (DPBS) instead of Hanks' balanced salt solution (HBSS) was used for CCF2-AM loading and washing steps for both conditions. As expected, the *rtxA1*::*bla* strain translocated Bla to HeLa cell cytosol in the presence of Ca^{2+}, although a significantly reduced proportion of cells (55.1% ± 2.2%) emitted blue fluorescence compared to the previous results (Fig. 6A, middle panels, compared to Fig. 3), possibly due to the use of DPBS. In contrast, cells treated in the absence of Ca^{2+} emitted no blue fluorescence (Fig. 6A, bottom panels). In addition, cells were not lysed by either the wild-type strain or the *rtxA1*::*bla* strain in the absence of Ca^{2+} (Fig. 6B).

These results initially suggested that $MARTX_{Vv}$ toxin translocation and cell lysis are Ca^{2+}-dependent processes. However, to ensure that the toxin was secreted under the DMEM growth conditions, nitrocefin cleavage assays were conducted with culture

supernatant fluids. When the Δ*rtxA1* or *rtxA1*::*bla* strain was grown in DMEM with Ca^{2+}, it was confirmed that supernatant fluids from *rtxA1*::*bla* cultures, but not Δ*rtxA1* cultures, exhibited Bla activity (Fig. 6C), consistent with the previous results conducted in LB media (Fig. 1C). However, when the Ca^{2+}-free media were used, the culture supernatant fluids from the *rtxA1*::*bla* strain no longer exhibited Bla activity (Fig. 6C), revealing that modified MARTX$_{Vv}$ toxin was absent from the culture medium (Fig. 6A and B). To distinguish whether the absence of modified MARTX$_{Vv}$ toxin in the medium was due to (i) lack of secretion or (ii) failure to synthesize toxin, total cell lysates of the *rtxA1*::*bla* strain grown in Ca^{2+}-free DMEM were tested and shown to carry Bla activity (Fig. 6D). These results indicate that the modified RtxA1::Bla toxin can be produced by *V. vulnificus* even in the absence of Ca^{2+}, albeit at lesser amounts, but that any synthesized toxin is not secreted into media. Therefore, the apparent defects in MARTX$_{Vv}$-dependent cell necrosis in Ca^{2+}-free media as previously described (19) are actually due to a defect of MARTX$_{Vv}$ toxin secretion and absence of toxin from the culture medium (Fig. 6C and D).

Repeat-containing regions are not responsible for rapid cell rounding. Prior to cell necrosis, one of the other obvious effects of the MARTX$_{Vv}$ toxin is cell rounding due to actin depolymerization (11). Indeed, HeLa cells are obviously rounded when treated with wild-type bacteria for only 30 min (Fig. 7C). The percentage of round cells increased with time, reaching nearly 100% by 120 min (Fig. 7A and C), when cells begin to lyse (Fig. 5A). By comparison, neither the Δ*rtxA1* strain nor the *rtxA1*::*bla* strain induced cell rounding through 120 min (Fig. 7C). Even at 210 min, when phenotypes of necrotic cell death, including swelling and blebbing, were apparent, cells treated with the *rtxA1*::*bla* strain were not rounded (Fig. 7B). These results indicate that (i) cell rounding is not a necessary prerequisite of MARTX$_{Vv}$-induced cell lysis and (ii) MARTX repeat-containing regions are not sufficient for cell rounding. Thus, in addition to a requirement for the repeat regions that mediate the translocation, the action of one or more MARTX effector domains must be required for this process. It is possible that the repeats and effector domain regions work together, especially if, for example, efflux of Ca^{2+} or K^+ through the pore activates eukaryotic cell signaling pathways that could contribute to cell rounding in concert with the action of the effector domain. Therefore, while necrotic cell death is dependent on the repeat-containing regions, other cytopathic activities, including rapid cell rounding, require the effector domain(s) in addition to the repeat regions.

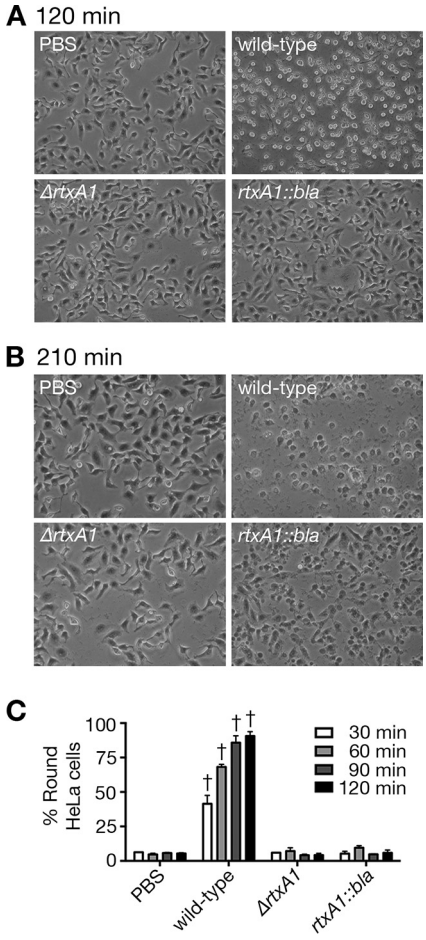

FIG 7 Rapid cell rounding by the MARTX$_{Vv}$ toxin requires effector domains. Representative images of HeLa cells treated with PBS or indicated *V. vulnificus* strains for 120 min (A) or 210 min (B) are shown. (C) Cell rounding was quantified every 30 min. Data are means ± standard deviations ($n = 3$) of the results determined for at least 50 (average, 75) cells per image. Only the cells showing a spherical shape were counted as positive. Statistical significance was determined by one-way ANOVA (†, $P < 0.001$).

DISCUSSION

MARTX toxins are large multifunctional toxins that range in size from 3,500 to 5,300 aa, with the variability determined by the number and size of the effector domains they carry. Sequence analysis using comparisons between toxins from different bacterial species has revealed that >300 kDa of the toxins are highly conserved (16). One of the highly conserved regions of the MARTX toxins is the C-terminal repeat region, which includes the nonapeptide RTX repeat motif [GGxG(N/D)Dx-hyd-x] that in other RTX toxins is known to bind to Ca^{2+}. In these other toxins, the tandemly ordered repeats are intrinsically disordered due to the electrostatic repulsions between negatively charged residues; the binding of Ca^{2+} to the conserved aspartate residues reduces this repulsion and consequently triggers folding of the RTX motif to form a beta-barrel structure (34–39). Thus, when the RTX repeats follow the ss through the TISS channel, relatively abundant Ca^{2+} in the extracellular environment binds to the aspartate residues triggering concomitant folding. The secreted, folded, and now stabilized RTX motif would prevent back import and facilitate continued export and folding of the holotoxin via a molecular ratchet mechanism (34–38). In fact, Ca^{2+}-dependent secretion has been suggested for other RTX toxins, including the *Bordetella pertussis* adenylate cyclase toxin and *Escherichia coli* pore-forming hemolysin (34–38).

By comparison to these other RTX toxins, the repeats in the carboxyl terminus of MARTX toxins have an atypical structure where an additional 9 to 11 aa are present between nonapeptide RTX repeats creating an 18 to 20 aa repeat (16). Although the aspartate residues predicted to bind calcium ion are strictly conserved in the MARTX repeats, their function(s) in Ca^{2+} binding has not as yet been examined. Here, using the modified MARTX$_{Vv}$ toxin containing the Bla reporter enzyme, we found that the secretion of MARTX$_{Vv}$ toxin is dependent on the carboxyl-terminal repeat-containing region (Fig. 1C) and that Ca^{2+} in the media was

also critical for the secretion of both the wild-type $MARTX_{Vv}$ toxin and the modified RtxA1::Bla toxin (Fig. 6). These results together suggest that the nonclassical RTX-like repeats in the carboxyl-terminal region of MARTX toxin may indeed bind to Ca^{2+} and thereby function in facilitating toxin secretion from the bacterium in a manner similar to other RTX toxins with the typical nonapeptide repeat.

Another proposed function of both the amino- and carboxyl-terminal repeat-containing regions of MARTX toxin is the formation of a pore or pore-like structure at the host cell membrane to translocate effector domains into the target eukaryotic cell cytosol (16). Indeed, using Bla as a reporter enzyme, we show that the repeat-containing regions have a heterologous protein translocation function (Fig. 2). Therefore, it is conceptually possible that any peptide that could be unfolded for secretion through the bacterial TISS could ultimately be translocated into a eukaryotic cell by the MARTX translocation platform. This translocation function was found to require the amino-terminal repeat-containing region (Fig. 1C and 3), indicating for the first time an importance of this region for MARTX-dependent effector domain translocation. We further speculate that the carboxyl-terminal repeat-containing region(s) is also critical for the effector domain translocation step, although, due to a block at the earlier step of toxin secretion, this could not be tested directly using the coculture system.

The autoprocessing CPD is another highly conserved feature of all MARTX toxins, so we explored whether CPD autoprocessing would be required for any step in cellular intoxication. Indeed, we found that the catalytic activity of CPD is dispensable for toxin secretion but is required for efficient Bla translocation (Fig. 4). This result might be explainable in two different ways. First, it is possible that the *rtxA1*::*bla cpd** strain translocates the same amount of Bla to host cells as the *rtxA1*::*bla* strain but that, in the absence of CPD autoprocessing activity, the toxin-tethered Bla can act only on a spatially restricted pool of near-membrane cytosolic CCF2. In such a case, the reduced amount of CCF2 cleavage in some cells may be insufficient for conversion above the necessary threshold to be detected as blue. Alternatively, if the action of the CPD at certain MARTX cleavage sites facilitates translocation of the remaining portion of the toxin to the host cytosol, reduced efficiency of the *rtxA1*::*bla cpd** strain may actually represent a reduced number of translocation events and thereby imply a coupling between MARTX autoprocessing and translocation.

The most important activity thus far linked to the MARTX holotoxin is its ability to induce cellular necrosis. This activity is thought to contribute to the breakdown of epithelial barriers, facilitating bacterial dissemination during infection. Studies employing transient expression of *rtxA1* fragments in epithelial cells had concluded that the portion of the $MARTX_{Vv}$ toxin sufficient for necrosis was comprised of only the CPD plus the carboxyl terminus (19). However, note that these conclusions were based on studies of toxin ectopically expressed within transfected eukaryotic cells rather than on that provided extracellularly. This is a critical distinction because the CPD from *V. cholerae* has been shown to induce apoptotic and necrotic cell death upon ectopic overexpression (40) but not when the CPD is transferred into cells via the natural route of intoxication as part of the $MARTX_{Vc}$ toxin (31, 41). In related results, the present study demonstrated that the protease activity of the $MARTX_{Vv}$ CPD does not contribute to epithelial necrosis when the toxin is delivered by coculture with bacterial cells (Fig. 5C). Further, we found that the amino terminus-truncated toxin cannot lyse epithelial cells (Fig. 5B). Indeed, our conclusion that the N terminus is essential for cellular necrosis is supported by a recent report that biochemically purified $MARTX_{Vv}$ comprised of only the CPD and the C-terminal region does not cause necrosis when added to cells (22), suggesting that in a purified system, the N terminus is also required. Note, however, that while the repeat regions are sufficient for necrosis, the modified toxin did show decreased efficiency in LDH release, indicating that the modification to the toxin likely structurally perturbed the translocation function of the pore.

Overall, our study has linked many of the activities of the $MARTX_{Vv}$ holotoxin to the repeat regions, including the ability to translocate effectors and induce cellular necrosis. Yet it is now clear that, while these repeat-containing regions are highly conserved (93% identical to $MARTX_{Vc}$ repeat regions), the ability of $MARTX_{Vv}$ to induce epithelial cell lysis is a unique feature of *V. vulnificus* and is not a function of the MARTX toxin of either *V. cholerae* or *V. anguillarum* (42, 43). Thus, unlike previous findings determined with *V. cholerae* (42), $MARTX_{Vv}$ toxin is a true membrane-damaging pore-forming toxin that also functions in translocation. In addition, it must have sufficient differences within its repeat-containing regions for this unique property of the $MARTX_{Vv}$ toxin compared to the MARTX toxins of either *V. cholerae* or *V. anguillarum*. The basis for these differences will require delving into the >300 kDa of peptide that comprises the repeat-containing regions to identify small but critical differences that can account for the alteration of function. This conceptually could be accomplished by genetic exchanges between the toxin genes from different species. However, this would generate hybrid toxins that could have the potential for increased toxicity and thus, for biosafety considerations, can be done only in a nonpathogenic host. The discovery of heterologous transfer of the small-domain Bla by a MARTX toxin has substantially reduced the predicted overall size of the *V. vulnificus rtxA1* gene such that attempts to clone and express recombinant toxins in nonpathogenic *E. coli*, which have thus far been futile, could potentially be revisited and generation of hybrid toxins in this genetic background might be possible.

Finally, a very important aspect of this study is that it also shows that the repeat regions cannot account for all the known functions of the holotoxin. In addition to necrosis, the toxin induces many cytopathic effects, including rapid actin depolymerization resulting in cell rounding (11). It is likely that rapid actin depolymerization has a critical role in pathogenesis since paralyzing phagocytes is a known consequence of *V. vulnificus* and has been documented in pathology studies of wound infections (44). We found that, despite its retaining the ability to induce obvious necrotic blebbing, the *rtxA1*::*bla* strain that encodes a toxin with no effector domains was not able to induce rapid cell rounding (Fig. 7B). Therefore, like $MARTX_{Vc}$ toxin, which carries multiple effectors known to regulate cytoskeletal dynamics resulting in destruction of the epithelial barrier and inhibition of phagocytosis (31), the $MARTX_{Vv}$ must also carry an effector domain(s) that modulates the cytoskeleton. A key candidate would be DUF5 or Rho-inactivation domain (RID), both of which have been shown by ectopic expression studies to induce cell rounding (45, 46). In addition, other domains of unknown function may be discovered to contribute. These data thus support the hypothesis that the

TABLE 2 Primers used in this study

Primer	Primer sequence, 5′→3′[a]
CL1	GCCAAAAACTCACTGGTTTAGG
CL2	GAAAGGAGCCCGAAGTAAGGTG
vvhA_For_1	AAAATATCTAGAGCCAAAAACTCACTGGTTTAGG
vvhA_Rev_1	AAAAAAGAGCTCGAAAGGAGCCCGAAGTAAGG
VvRtxA-Bla-3	AAAGTCGACTCATGCGAAGTTTCACCAAG
VvRtxA-Bla-4	AGAGCTCGGTGAAAGAAGAGTCGGAAGC
VvRtxA-Bla-1	ATCTAGAACTTTGTTGTTTTCTGCTTTTTGG
VvRtxA-Bla-2	AAAGTCGACCAAAGGGATTGAAGGGTTC
pBLUE-Bla-SX1	AAACTCGAGTACCAATGCTTAATCAGTG
pBLUE-Bla-SX2	AAAGTCGACAATGAGTATTCAACATTTCCG
dRtxB constructF	ACTGGCATGCCACAAGCTCGCTTTGACATCACTT GGTTC
dRtxB constructR	ACTGGAGCTCTCATGCGGTGGTTTCCTCTTGTTTG

[a] Regions of primers not complementary to corresponding genes are underlined.

$MARTX_{Vv}$ toxin is a truly multifunctional toxin: the repeat-containing regions function for effector domain delivery from bacteria to the cell cytosol and for epithelial cell lysis, while effector domains are required for other cytopathic effects of the toxin such as actin depolymerization.

MATERIALS AND METHODS

Ethics statement. This study was carried out in strict accordance with the recommendations in the U.S. Public Health Service regulations and applicable federal and local laws. All recombinant methods for generation of modified toxins were approved by the Northwestern University Institutional Biological Safety Committee.

Bacterial strains and cell culture. The plasmids and bacterial strains used in this study are listed in Table 1. Unless noted otherwise, *V. vulnificus* and *E. coli* strains were grown in Luria-Bertani (LB) broth and agar supplemented with 50 μg/ml rifampin or 10 μg/ml chloramphenicol, as needed. Bacterial growth in LB media was monitored using a Beckman DU530 spectrophotometer. Unless noted otherwise, HeLa cells were cultured at 37°C with 5% CO_2 in DMEM containing 10% fetal bovine serum (FBS), 50 μg/ml penicillin, and 50 μg/ml streptomycin. All reagents and chemicals were purchased from Sigma or Life Technologies, except nitrocefin, which was obtained from EMD Millipore. Restriction enzymes were purchased from New England Biolabs. Plasmid DNA was isolated using Epoch Biolabs Econospin spin columns and sequenced in the Northwestern University Genomics core facility. Primers (Table 2) and Gblocks were obtained from Integrated DNA Technologies (Coralville, IA).

Generation of *sacB*-counterselectable plasmids for deletion within *vvhA*. To generate a genetic background that does not secrete the cytolysin VvhA, *vvhA* and flanking sequences were first amplified from the CMCP6 chromosomal DNA template using primers CL1 and CL2. The 2,027-bp product was captured in plasmid pCR-TOPO-Blunt and sequenced. The plasmid was digested with HpaI sites and religated, creating an in-frame removal of 972 bp from *vvhA*. Following our standard protocol for *V. cholerae* (47), the fragment was originally moved into *sacB*-counterselectable plasmid pWM91 and integrated into CMCP6, but this plasmid was found to not properly resolve in *V. vulnificus* upon sucrose selection. The deletion fragment was thus reamplified from the cointegrate strain using vvhA_For_1 and vvhA_Rev_1 primers and ligated into alternative vector pDS132 using the XbaI and SacI sites. This pBS1311 vector was exchanged into rifampin-resistant CMCP6 as described below.

Generation of *sacB*-counterselectable plasmids for alterations to *rtxA1*. To generate the *rtxA1*::*bla* plasmid, 833 bp corresponding to the end of the amino-terminal repeat-containing region of *rtxA1* was amplified by PCR using primers VvRtxA-Bla-3 and VvRtxA-Bla-4, and 786 bp corresponding to the carboxyl-terminal region, including *cpd* of *rtxA1*, was amplified using primers VvRtxA-Bla-1 and VvRtxA-Bla-2. The fragments treated with restriction enzymes were assembled into the SacI-XbaI sites of *SacB*-counterselectable plasmid pDS132 (48), generating a unique SalI site between the two fragments. Primers pBLUE-Bla-SX1 and pBLUE-Bla-SX2 were used to amplify the 861 bp of *bla* from pBlueScript-II (Stratagene, USA), which was then ligated into the unique SalI site, creating pHGJ5. After the insertion was sequenced for accuracy, the plasmid was transformed to SM10λpir.

To generate the large deletion at the 5′ end of *rtxA1*::*bla*, two 500-bp double-stranded synthetic gBlocks corresponding to upstream and downstream flanking regions of *rtxA1*::*bla* bp 217 to 5655 were assembled into SphI-SacI-digested pDS132 using Gibson Assembly master mix (New England Biolabs) at 50°C. After confirmation of the insertion sequence, the resulting pBS1347 plasmid was transformed to S17-1λ*pir*.

Similarly, the large deletion at the 3′ end of *rtxA1*::*bla* was generated using gBlocks corresponding to upstream or downstream flanking regions of *rtxA1*::*bla* bp 7597 to 9879 and SphI-SacI-digested pDS132. The resulting assembled pBS1348 plasmid was sequenced for insertion accuracy and then transformed to S17-1λ*pir*.

To generate the *rtxA1*::*bla*::*cpd** strain, one 500-bp double-stranded synthetic gBlock was assembled into SphI-SacI-digested pDS132 vector using Gibson Assembly master mix at 50°C. This gBlock insertion was designed to include a codon change of the catalytic C4230 residue of CPD to Ala. The resulting pHEG1401 plasmid was sequenced for accuracy and then transformed to SM10λ*pir*.

To generate an insertional disruption in *rtxB*, 1,742 bp of the internal region of *rtxB* was amplified by PCR using primers dRtxB-Construct-F and dRtxB-Construct-R. The amplified fragment treated with restriction enzymes was ligated into the SphI and SacI sites of pDS132. The resulting plasmid was digested with NheI, treated with Klenow fragment of DNA polymerase I, and then ligated to an *nptII* cassette isolated from the pKanπ vector by digestion with HincII. The resulting pBS1438 plasmid was confirmed for *nptII* insertion by PCR and then transformed to S17-1λ*pir*.

Plasmids pBS1311, pHGJ5, pBS1347, pBS1348, pHEG1401, and pBS1438 were transferred to *V. vulnificus* strains by conjugation followed by selection for double homologous recombination using sucrose counterselection to isolate recombinants as previously described (47).

Nitrocefin cleavage assay. *V. vulnificus* strains were grown in triplicate cultures in LB to the exponential phase, and 90 μl of whole bacterial cultures was incubated with 10 μl of nitrocefin (1 mg/ml in PBS) for 3 h at room temperature. Absorbance (A_{486}) of cleaved nitrocefin was measured at the indicated time points using a SpectraMax M5 plate reader (Molecular Devices).

For some assays, *V. vulnificus* grown overnight in LB was washed with PBS and inoculated into DMEM with or without 1.8 mM $CaCl_2$. After static incubation at 37°C in 5% CO_2 until bacterial cultures reached the exponential phase (optical density at 600 nm [OD_{600}] = 0.5), bacteria were pelleted by centrifugation at 2,800 × *g* in 4°C for 20 min. Supernatant fluids were kept on ice until used. Cell pellets were washed with 10 mM Tris buffer (pH 8.0) and then resuspended in ice-cold water, sonicated, and then adjusted to reach concentrations of 20 mM Tris and 1 mM EDTA (pH 8.0). Lysates were centrifuged at 20,000 × *g* in 4°C for 30 min. Cell lysates and supernatant fluids were assayed as described for whole bacterial culture.

Antibiotic disk assay. Fresh LB agar plates were swabbed with exponential-phase cultures of the indicated strains, and a 6.5-mm-diameter ceftazidime (CAZ) antibiotic disk (Thermo Scientific) was sterilely placed in the center of each plate. Plates were incubated inverted at 30°C overnight. The area (A) of the clear zone of inhibition around the disk was quantified as $A = \pi(0.5d)^2 - A_{disk}$, where d is the measured diameter of the zone and A_{disk} is 33.18 mm^2.

***In vitro* translocation assay.** A total of 5×10^5 HeLa cells were seeded into 12-well dishes overnight. Exponential-phase, PBS-washed *V. vulnificus* was added to cells at an MOI of 10 unless indicated otherwise. Plates were centrifuged at 500 × *g* for 5 min and then incubated at 37°C in 5% CO_2 for 60 min unless indicated otherwise. The cells were then washed

with HBSS or DPBS and loaded with CCF2-AM for 30 min in the dark. Stained cells were suspended in HBSS flow buffer (1× HBSS, 0.5 mM EDTA, 25 mM HEPES, 2% bovine serum albumin [BSA], pH 7.4) and transferred to ice. Flow cytometry of a minimum of 10,000 events per sample was performed on a BD Biosciences (Heidelberg, Germany) FACSCanto II system with excitation at 405 nm (violet), using fluorescence-activated cell sorter (FACS) Diva software. AmCyan 450/50 and Pacific Blue 510/50 emission filters were used for the collection of data. To eliminate cell debris, first, all events were gated using forward scatter (FSC) and side scatter (SSC) and then intact cell events were applied. FACS gates for green and blue fluorescence were set using the analyzed data from uninfected, CCF2/AM-loaded HeLa cells.

LDH release assay. HeLa cells were seeded into 6-well dishes to a density of 10^5 cells per well overnight. The media were exchanged for 3 ml of phenol-red free or calcium-free DMEM, without FBS and penicillin-streptomycin, and *V. vulnificus* strains were added at an MOI of 10. LDH release to media at the indicated times was measured using a CytoTox 96 nonradioactive cytotoxicity assay kit (Promega, Madison, WI) according to the manufacturer's instructions. Percent cell lysis was calculated as A_{490} (sample)/A_{490} (100% lysis control) × 100.

Cell rounding assay. HeLa cells were seeded into 6-well dishes to a density of 10^5 cells per well overnight. The media were exchanged for 3 ml of phenol-red free DMEM without FBS and penicillin-streptomycin, and PBS or the indicated *V. vulnificus* strains were added at an MOI of 10. Images for random spots of the culture wells were taken through a microscope every 30 min using a digital camera (Nikon Eclipse TS100; ×10 magnification). Percentages of round cells were calculated as the number of round cells in an image/the total number of cells in an image × 100.

Statistical analysis. Statistical analyses were performed as noted in the figure legends using GraphPad Prism 6.0 for MacIntosh software (San Diego, CA).

ACKNOWLEDGMENTS

We thank Jazel Salle Dolores for assistance on flow cytometry and Kevin Ziolo, Jennifer Wong, and Chris Lowe for technical assistance. Core services were provided by the Northwestern Genomics Core and the flow cytometry facility of the Northwestern Interdepartmental Immunobiology Center.

This work was supported by National Institutes of Health grants R01 AI092825 and R01 AI098369, an Investigators in the pathogenesis of Infectious Diseases award from the Burroughs Wellcome Fund, and the Northwestern Medicine Catalyst Fund (to K.J.F.S.). B.S.K. was supported by Basic Science Research Program through the National Research Foundation of Korea funded by the Ministry of Education, Science and Technology (NRF-2013R1A6A3A03024337). H.E.G. was supported by the Ruth L. Kirschestein NRSA Cellular and Molecular Basis of Disease Training Grant at Northwestern University (T32 GM08061).

REFERENCES

1. **Blake PA, Merson MH, Weaver RE, Hollis DG, Heublein PC.** 1979. Disease caused by a marine *Vibrio*. Clinical characteristics and epidemiology. N Engl J Med **300:**1–5. http://dx.doi.org/10.1056/NEJM197901043000101.
2. **Linkous DA, Oliver JD.** 1999. Pathogenesis of *Vibrio vulnificus*. FEMS Microbiol Lett **174:**207–214. http://dx.doi.org/10.1111/j.1574-6968.1999.tb13570.x.
3. **Gulig PA, Bourdage KL, Starks AM.** 2005. Molecular pathogenesis of *Vibrio vulnificus*. J Microbiol **43**(Spec No)118–131.
4. **Strom MS, Paranjpye RN.** 2000. Epidemiology and pathogenesis of *Vibrio vulnificus*. Microbes Infect **2:**177–188. http://dx.doi.org/10.1016/S1286-4579(00)00270-7.
5. **Menon MP, Yu PA, Iwamoto M, Painter J.** 2014. Pre-existing medical conditions associated with *Vibrio vulnificus* septicaemia. Epidemiol Infect **142:**878–881. http://dx.doi.org/10.1017/S0950268813001593.
6. **Jeong HG, Satchell KJ.** 2012. Additive function of *Vibrio vulnificus* MARTX(Vv) and VvhA cytolysins promotes rapid growth and epithelial tissue necrosis during intestinal infection. PLoS Pathog **8:**e1002581. http://dx.doi.org/10.1371/journal.ppat.1002581.
7. **Lo HR, Lin JH, Chen YH, Chen CL, Shao CP, Lai YC, Hor LI.** 2011. RTX toxin enhances the survival of *Vibrio vulnificus* during infection by protecting the organism from phagocytosis. J Infect Dis **203:**1866–1874. http://dx.doi.org/10.1093/infdis/jir070.
8. **Ziolo KJ, Jeong HG, Kwak JS, Yang S, Lavker RM, Satchell KJ.** 2014. *Vibrio vulnificus* biotype 3 MARTX toxin is an adenylate cyclase toxin essential for virulence in mice. Infect Immun **82:**2148–2157. http://dx.doi.org/10.1128/IAI.00017-14.
9. **Liu M, Alice AF, Naka H, Crosa JH.** 2007. The HlyU protein is a positive regulator of rtxA1, a gene responsible for cytotoxicity and virulence in the human pathogen *Vibrio vulnificus*. Infect Immun **75:**3282–3289. http://dx.doi.org/10.1128/IAI.00045-07.
10. **Lee JH, Kim MW, Kim BS, Kim SM, Lee BC, Kim TS, Choi SH.** 2007. Identification and characterization of the *Vibrio vulnificus rtxA* essential for cytotoxicity *in vitro* and virulence in mice. J Microbiol **45:**146–152.
11. **Kim YR, Lee SE, Kook H, Yeom JA, Na HS, Kim SY, Chung SS, Choy HE, Rhee JH.** 2008. *Vibrio vulnificus* RTX toxin kills host cells only after contact of the bacteria with host cells. Cell Microbiol **10:**848–862. http://dx.doi.org/10.1111/j.1462-5822.2007.01088.x.
12. **Fan JJ, Shao CP, Ho YC, Yu CK, Hor LI.** 2001. Isolation and characterization of a *Vibrio vulnificus* mutant deficient in both extracellular metalloprotease and cytolysin. Infect Immun **69:**5943–5948. http://dx.doi.org/10.1128/IAI.69.9.5943-5948.2001.
13. **Kim YR, Lee SE, Kim CM, Kim SY, Shin EK, Shin DH, Chung SS, Choy HE, Progulske-Fox A, Hillman JD, Handfield M, Rhee JH.** 2003. Characterization and pathogenic significance of *Vibrio vulnificus* antigens preferentially expressed in septicemic patients. Infect Immun **71:**5461–5471. http://dx.doi.org/10.1128/IAI.71.10.5461-5471.2003.
14. **Kwak JS, Jeong HG, Satchell KJ.** 2011. *Vibrio vulnificus* rtxA1 gene recombination generates toxin variants with altered potency during intestinal infection. Proc Natl Acad Sci U S A **108:**1645–1650. http://dx.doi.org/10.1073/pnas.1014339108.
15. **Roig FJ, González-Candelas F, Amaro C.** 2011. Domain organization and evolution of multifunctional autoprocessing repeats-in-toxin (MARTX) toxin in *Vibrio vulnificus*. Appl Environ Microbiol **77:**657–668. http://dx.doi.org/10.1128/AEM.01806-10.
16. **Satchell KJ.** 2011. Structure and function of MARTX toxins and other large repetitive RTX proteins. Annu Rev Microbiol **65:**71–90. http://dx.doi.org/10.1146/annurev-micro-090110-102943.
17. **Shen A, Lupardus PJ, Albrow VE, Guzzetta A, Powers JC, Garcia KC, Bogyo M.** 2009. Mechanistic and structural insights into the proteolytic activation of *Vibrio cholerae* MARTX toxin. Nat Chem Biol **5:**469–478. http://dx.doi.org/10.1038/nchembio.178.
18. **Chung KJ, Cho EJ, Kim MK, Kim YR, Kim SH, Yang HY, Chung KC, Lee SE, Rhee JH, Choy HE, Lee TH.** 2010. RtxA1-induced expression of the small GTPase Rac2 plays a key role in the pathogenicity of *Vibrio vulnificus*. J Infect Dis **201:**97–105. http://dx.doi.org/10.1086/648612.
19. **Kim YR, Lee SE, Kang IC, Nam KI, Choy HE, Rhee JH.** 2013. A bacterial RTX toxin causes programmed necrotic cell death through calcium-mediated mitochondrial dysfunction. J Infect Dis **207:**1406–1415. http://dx.doi.org/10.1093/infdis/jis746.
20. **Toma C, Higa N, Koizumi Y, Nakasone N, Ogura Y, McCoy AJ, Franchi L, Uematsu S, Sagara J, Taniguchi S, Tsutsui H, Akira S, Tschopp J, Núñez G, Suzuki T.** 2010. Pathogenic *Vibrio* activate NLRP3 inflammasome via cytotoxins and TLR/nucleotide-binding oligomerization domain-mediated NF-kappa B signaling. J Immunol **184:**5287–5297. http://dx.doi.org/10.4049/jimmunol.0903536.
21. **Lee BC, Choi SH, Kim TS.** 2008. *Vibrio vulnificus* RTX toxin plays an important role in the apoptotic death of human intestinal epithelial cells exposed to Vibrio vulnificus. Microbes Infect **10:**1504–1513. http://dx.doi.org/10.1016/j.micinf.2008.09.006.
22. **Lee TH, Kim MH, Lee CS, Lee JH, Rhee JH, Chung KM.** 2014. Protection against *Vibrio vulnificus* infection by active and passive immunization with the C-terminal region of the RtxA1/MARTXVv protein. Vaccine **32:**271–276. http://dx.doi.org/10.1016/j.vaccine.2013.11.019.
23. **Charpentier X, Oswald E.** 2004. Identification of the secretion and translocation domain of the enteropathogenic and enterohemorrhagic Escherichia coli effector Cif, using TEM-1 beta-lactamase as a new fluorescence-based reporter. J Bacteriol **186:**5486–5495. http://dx.doi.org/10.1128/JB.186.16.5486-5495.2004.
24. **Zlokarnik G, Negulescu PA, Knapp TE, Mere L, Burres N, Feng L,**

Whitney M, Roemer K, Tsien RY. 1998. Quantitation of transcription and clonal selection of single living cells with beta-lactamase as reporter. Science **279:**84–88. http://dx.doi.org/10.1126/science.279.5347.84.

25. **Geddes K, Cruz F, Heffron F**. 2007. Analysis of cells targeted by *Salmonella* type III secretion in vivo. PLoS Pathog **3:**e196. http://dx.doi.org/10.1371/journal.ppat.0030196.
26. **Prochazkova K, Shuvalova LA, Minasov G, Voburka Z, Anderson WF, Satchell KJ**. 2009. Structural and molecular mechanism for autoprocessing of MARTX toxin of *Vibrio cholerae* at multiple sites. J Biol Chem **284:**26557–26568. http://dx.doi.org/10.1074/jbc.M109.025510.
27. **Yamamoto K, Ichinose Y, Shinagawa H, Makino K, Nakata A, Iwanaga M, Honda T, Miwatani T**. 1990. Two-step processing for activation of the cytolysin/hemolysin of *Vibrio cholerae* O1 biotype El Tor: nucleotide sequence of the structural gene (hlyA) and characterization of the processed products. Infect Immun **58:**4106–4116.
28. **Lee BC, Lee JH, Kim MW, Kim BS, Oh MH, Kim KS, Kim TS, Choi SH**. 2008. *Vibrio vulnificus* rtxE is important for virulence, and its expression is induced by exposure to host cells. Infect Immun **76:**1509–1517. http://dx.doi.org/10.1128/IAI.01503-07.
29. **Horseman MA, Surani S**. 2011. A comprehensive review of *Vibrio vulnificus*: an important cause of severe sepsis and skin and soft-tissue infection. Int J Infect Dis **15:**e157–e166. http://dx.doi.org/10.1016/j.ijid.2010.11.003.
30. **Palzkill T, Botstein D**. 1992. Identification of amino acid substitutions that alter the substrate specificity of TEM-1 beta-lactamase. J Bacteriol **174:**5237–5243.
31. **Dolores JS, Agarwal S, Egerer M, Satchell KJ**. 2015. *Vibrio cholerae* MARTX toxin heterologous translocation of beta-lactamase and roles of individual effector domains on cytoskeleton dynamics. Mol Microbiol **95:**590–604. http://dx.doi.org/10.1111/mmi.12879.
32. **Chumbler NM, Farrow MA, Lapierre LA, Franklin JL, Haslam DB, Goldenring JR, Lacy DB**. 2012. *Clostridium difficile* toxin B causes epithelial cell necrosis through an autoprocessing-independent mechanism. PLoS Pathog **8:**e1003072. http://dx.doi.org/10.1371/journal.ppat.1003072.
33. **Li S, Shi L, Yang Z, Feng H**. 2013. Cytotoxicity of *Clostridium difficile* toxin B does not require cysteine protease-mediated autocleavage and release of the glucosyltransferase domain into the host cell cytosol. Pathog Dis **67:**11–18. http://dx.doi.org/10.1111/2049-632X.12016.
34. **Chenal A, Guijarro JI, Raynal B, Delepierre M, Ladant D**. 2009. RTX calcium binding motifs are intrinsically disordered in the absence of calcium: implication for protein secretion. J Biol Chem **284:**1781–1789. http://dx.doi.org/10.1074/jbc.M807312200.
35. **Sotomayor Pérez AC, Karst JC, Davi M, Guijarro JI, Ladant D, Chenal A**. 2010. Characterization of the regions involved in the calcium-induced folding of the intrinsically disordered RTX motifs from the *Bordetella pertussis* adenylate cyclase toxin. J Mol Biol **397:**534–549. http://dx.doi.org/10.1016/j.jmb.2010.01.031.
36. **Blenner MA, Shur O, Szilvay GR, Cropek DM, Banta S**. 2010. Calcium-induced folding of a beta roll motif requires C-terminal entropic stabilization. J Mol Biol **400:**244–256. http://dx.doi.org/10.1016/j.jmb.2010.04.056.
37. **Thomas S, Bakkes PJ, Smits SH, Schmitt L**. 2014. Equilibrium folding of pro-HlyA from *Escherichia coli* reveals a stable calcium ion dependent folding intermediate. Biochim Biophys Acta **1844:**1500–1510. http://dx.doi.org/10.1016/j.bbapap.2014.05.006.
38. **Sotomayor-Perez AC, Ladant D, Chenal A**. 2014. Disorder-to-order transition in the CyaA toxin RTX domain: implications for toxin secretion. Toxins (Basel) **7:**1–20. http://dx.doi.org/10.3390/toxins7010001.
39. **Baumann U, Wu S, Flaherty KM, McKay DB**. 1993. Three-dimensional structure of the alkaline protease of *Pseudomonas aeruginosa*: a two-domain protein with a calcium binding parallel beta roll motif. EMBO J **12:**3357–3364.
40. **Sheahan KL, Cordero CL, Satchell KJ**. 2007. Autoprocessing of the *Vibrio cholerae* RTX toxin by the cysteine protease domain. EMBO J **26:**2552–2561. http://dx.doi.org/10.1038/sj.emboj.7601700.
41. **Ahrens S, Geissler B, Satchell KJ**. 2013. Identification of a His–Asp–Cys catalytic triad essential for function of the Rho inactivation domain (RID) of *Vibrio cholerae* MARTX toxin. J Biol Chem **288:**1397–1408. http://dx.doi.org/10.1074/jbc.M112.396309.
42. **Fullner KJ, Mekalanos JJ**. 2000. *In vivo* covalent crosslinking of actin by the RTX toxin of *Vibrio cholerae*. EMBO J **19:**5315–5323. http://dx.doi.org/10.1093/emboj/19.20.5315.
43. **Li L, Rock JL, Nelson DR**. 2008. Identification and characterization of a repeat-in-toxin gene cluster in *Vibrio anguillarum*. Infect Immun **76:**2620–2632. http://dx.doi.org/10.1128/IAI.01308-07.
44. **Starks AM, Bourdage KL, Thiaville PC, Gulig PA**. 2006. Use of a marker plasmid to examine differential rates of growth and death between clinical and environmental strains of *Vibrio vulnificus* in experimentally infected mice. Mol Microbiol **61:**310–323. http://dx.doi.org/10.1111/j.1365-2958.2006.05227.x.
45. **Sheahan KL, Satchell KJ**. 2007. Inactivation of small Rho GTPases by the multifunctional RTX toxin from *Vibrio cholerae*. Cell Microbiol **9:**1324–1335. http://dx.doi.org/10.1111/j.1462-5822.2006.00876.x.
46. **Antic I, Biancucci M, Satchell KJ**. 2014. Cytotoxicity of the *Vibrio vulnificus* MARTX toxin effector DUF5 is linked to the C2A subdomain. Proteins **82:**2643–2656. http://dx.doi.org/10.1002/prot.24628.
47. **Fullner KJ, Mekalanos JJ**. 1999. Genetic characterization of a new type IV pilus gene cluster found in both classical and El Tor biotypes of *Vibrio cholerae*. Infect Immun **67:**1393–1404.
48. **Philippe N, Alcaraz JP, Coursange E, Geiselmann J, Schneider D**. 2004. Improvement of pCVD442, a suicide plasmid for gene allele exchange in bacteria. Plasmid **51:**246–255. http://dx.doi.org/10.1016/j.plasmid.2004.02.003.
49. **Miller VL, Mekalanos JJ**. 1988. A novel suicide vector and its use in construction of insertion mutations: osmoregulation of outer membrane proteins and virulence determinants in *Vibrio cholerae* requires toxR. J Bacteriol **170:**2575–2583.
50. **Simon R, Priefer U, Pühler A**. 1983. A broad host range mobilization system for in vivo genetic engineering: transposon mutagenesis in gram negative bacteria. Nat Biotechnol **1:**784–791. http://dx.doi.org/10.1038/nbt1183-784.